



# **Geophysical Research Letters**\*

# <del>-</del>

# RESEARCH LETTER

10.1029/2023GL107889

#### **Key Points:**

- Azimuthally propagating "auroral curls" with mesoscale wavelengths were observed in Antarctica
- These curls are fine structures in the poleward boundary of multiple arcs formed by longitudinal-arranged fieldaligned current pairs
- Ionospheric flow velocities nearby oscillate with periods in the Pc 5 band, indicating connections with ultra-low frequency waves

#### **Supporting Information:**

Supporting Information may be found in the online version of this article.

#### Correspondence to:

Q.-G. Zong, qgzong@pku.edu.cn

#### Citation:

Li, X.-Y., Zong, Q.-G., Hu, Z.-J., Wang, Y.-F., Liu, J.-J., Zhou, X.-Z., et al. (2024). Mesoscale auroral curls in Antarctica. Geophysical Research Letters, 51, e2023GL107889. https://doi.org/10.1029/2023GL107889

Received 19 DEC 2023 Accepted 18 FEB 2024

# © 2024. The Authors. This is an open access article under the terms of the Creative Commons Attribution-NonCommercial-NoDerivs License, which permits use and distribution in any medium, provided the original work is properly cited, the use is non-commercial and no modifications or adaptations are made.

# **Mesoscale Auroral Curls in Antarctica**

Xing-Yu Li<sup>1</sup>, Qiu-Gang Zong<sup>1,2</sup>, Ze-Jun Hu<sup>3</sup>, Yong-Fu Wang<sup>1</sup>, Jian-Jun Liu<sup>3</sup>, Xu-Zhi Zhou<sup>1</sup>, Chao Yue<sup>1</sup>, Shan Wang<sup>1</sup>, Zi-Kang Xie<sup>1,3</sup>, Xing-Xin Zhao<sup>1,3</sup>, Zhi-Yang Liu<sup>4</sup>, Ze-Fan Yin<sup>1,3</sup>, Hua-Yu Zhao<sup>3</sup>, and Yi-Xin Sun<sup>1</sup>

<sup>1</sup>Institute of Space Physics and Applied Technology, Peking University, Beijing, China, <sup>2</sup>State Key Laboratory of Lunar and Planetary Sciences, Macau University of Science and Technology, Taipa, Macau, China, <sup>3</sup>Antarctic Zhongshan National Field Observation and Research Station for Snow and Ice, Space Special Environment and Disasters, Polar Research Institute of China, Shanghai, China, <sup>4</sup>Institut de Recherche en Astrophysique et Planétologie, CNES-CNRS-Universite Toulouse III Paul Sabatier, Toulouse, France

**Abstract** The morphology and motion of auroras have been widely studied due to their indications on magnetospheric processes. Here, we report a new kind of "auroral curls," which have wavelengths in the mesoscale (~100 km) and propagate azimuthally. Utilizing data from the Chinese Antarctic Zhongshan Station (the all-sky imager and the high-frequency radar), the Active Magnetosphere and Planetary Electrodynamics Response Experiment and the Defense Meteorological Satellite Program, we analyze an event occurred on 23 April 2019. We find these curls are fine structures in the poleward boundary of multiple arcs. Corresponding field-aligned currents manifest as a series of longitudinally arranged pairs, while ionospheric flow velocities nearby oscillate with periods in the Pc 5 band. Observational evidence suggests these curls are connected with ultra-low frequency (ULF) waves, which opens the possibility of using auroras to globally image ULF waves.

**Plain Language Summary** Auroras caused by precipitation of magnetospheric particles contain information about physical processes happened in the magnetosphere. In this letter, we report a new kind of auroral dynamic forms observed in Antarctica. These structures present both spatial and temporal periodic characteristics, which have similar scales with those of magnetospheric ultra-low frequency (ULF) waves. We propose these auroral forms are connected with ULF waves, which provides a potential method to globally image ULF waves by analyzing properties of these auroras.

#### 1. Introduction

Auroras are a common phenomenon that occur in high latitudes of planets (Hu et al., 2009). As a visible space-physical phenomenon, they have garnered widespread attention over the past few decades (e.g., Frey, 2007; Karlsson et al., 2020; Nishimura et al., 2020). These emissions originate from magnetospheric particle precipitation. Therefore, many studies (e.g., Akasofu, 1964; Keiling et al., 2009; Yue et al., 2013) have utilized imaging observations of auroral morphology and motion to infer the physical processes occurring within the magnetosphere.

In previous investigations, the formation of multi-scale periodic signatures in auroras remains an open question. It is proposed to be connected with multiple mechanisms (Kataoka et al., 2021). For example, the vortex-like structures along auroral arcs can be categorized into "spirals," "folds," "curls" and "ruffs" based on their spatial scales, lifetimes and vorticities. Spirals have diameters ranging from 20 to 1,300 km (Davis & Hallinan, 1976), which are explained as results of magnetic field line distortions at the free end (Hallinan, 1976) caused by field-aligned currents (FACs). Folds have typical scales of ~20 km (Kataoka et al., 2011). Simulation work suggests they are related to the non-linear evolution of plasma instabilities and inertial Alfvén waves (e.g., Chaston & Seki, 2010; Chmyrev et al., 1992; Wagner et al., 1983). Curls are smaller-size (kilometer-scale) structures manifesting as a series of vortices. The Kelvin-Helmholtz (K-H) instability relevant to flow shear (Vogt et al., 1999) across negatively (e.g., Miura & Sato, 1978) or positively (e.g., Kimball & Hallinan, 1998) charged field-aligned sheets is believed to contribute to the production of curls. Ruffs are recently found finer ( < 3 km) distortions along curls (Dahlgren et al., 2010). They exhibit inverse rotation with curls and their formation mechanisms are still unclear.

For some auroral forms, they display the periodicity in Pc 3–5 range (10–600 s, Jacobs et al., 1964), thus suggesting an association with ultra-low frequency (ULF) waves within the same band. ULF waves in Pc 3–5 bands

are widely distributed magneto-hydro-dynamic waves in the magnetosphere (e.g., Baker et al., 2003; Liu et al., 2009; Zong, 2022). These waves can efficiently exchange energy with charged particles (e.g., Li et al., 2021, 2022; Liu et al., 2020; Oimatsu et al., 2018; Southwood & Kivelson, 1981; Southwood & Kivelson, 1982; Yamamoto et al., 2019; Zong et al., 2009, 2017), regulating the energy transport throughout the entire solar wind-magnetosphere-ionosphere coupling system. In prior observations, the effects of ULF waves primarily manifested as temporal modulations of auroras. In light of concurrent geomagnetic and optical measurements (e.g., Gillies et al., 2018; Milan et al., 2001; Yin, Zhou, Hu, et al., 2023), the generation of poleward-moving auroral arcs with minute-scale periodic recurrence is attributed to field line resonances (FLRs). Theoretical work of FLRs (e.g., Rankin, Samson, & Tikhonchuk, 1999; Rankin, Samson, Tikhonchuk, & Voronkov, 1999; Streltsov & Lotko, 2008) suggests they can establish parallel electric fields in high latitudes and accelerate electrons to produce periodic arcs. Besides, ULF waves can modulate the emission of lower-band chorus waves and electrostatic electron cyclotron harmonic waves, periodically scattering energetic electrons into the loss cone, thereby giving rise to pulsating auroras (e.g., Li et al., 2023; Motoba et al., 2019; Motoba et al., 2021). ULF waves can also induce direct particle precipitation by altering the size of the loss cone (Rae et al., 2018) or the altitude of the mirror point (Yin, Zhou, Li, et al., 2023). Nonetheless, there is limited research on how ULF waves affect the formation of spatial periodic auroral structures.

In this letter, we report a new form of "auroral curls" which is possibly related to ULF waves. These curls have azimuthal wavelength in the mesoscale ( $\sim$ 30–500 km, which corresponds to the scale in the order of the Earth's radius in the magnetospheric equatorial plane) (e.g., Gabrielse et al., 2018; Keesee et al., 2021). Observations from multiple instruments were used to analyze their structures, including ground-based optical and radar detection, along with spaceborne in-situ measurements. We propose these spatial periodic auroral forms could be induced by ULF waves, which offers a new approach to globally visualize ULF waves using auroral observations.

#### 2. Observations

In this study, we analyzed ground-based auroral imaging data obtained by the all-sky imager (ASI) at the Chinese Antarctic Zhongshan Station (ZHS). ZHS is located at (-74.66°S, 96.80°E) in corrected geomagnetic coordinates, which makes it capable to observe the nightside, the post-noon and the cusp dayside auroras (Hu et al., 2017). The Magnetic Local Time (MLT) of ZHS is approximately equal to UT +1.75 hr. An advanced synthetic auroral observation system has been conducting observations since 2010, which includes a multiwavelength all-sky auroral imaging observation component with six interference filters centered at 427.8, 432.0, 540.0, 557.7, 620.0 and 630.0 nm respectively. We used auroral images in the 557.7 and 630.0 nm wavebands, which mainly correspond to electron precipitation with energies of 0.5 to a few keV and less than 500 eV (Hu et al., 2009). The temporal resolution of the ASI data is 10 s (exposure time: 4 s). The diameter of the field-of-view (FOV) is about 1,000 km at an altitude of 150 km. Ionospheric flow data measured by the high frequency (HF) radar at ZHS (10.2-10.4 MHz) are used as well, which is a part of the Super Dual Auroral Radar Network (SuperDARN, Chisham et al., 2007) with the code "ZHO." This radar scans through 16 uniformly distributed beams with an azimuthal separation of ~3.24° and produces a fan-shaped FOV map every minute (Chen et al., 2022; Greenwald et al., 1985, 1995). For each beam, the dwell time is 3 s and 75 range gates are sampled with a gate length of 45 km (Liu et al., 2011; Jiang et al., 2022). The ZHO radar has two channels performing different scanning patterns at the same time (Hu et al., 2013; Liu et al., 2013). One channel operates a fixed-frequency mode with all beams, while the other one performs a sweep-frequency mode with a single beam (beam-07). Here we present data from the single-beam channel as they have higher temporal resolutions (3 s).

We also used data from the Active Magnetosphere and Planetary Electrodynamics Response Experiment (AMPERE, Anderson et al., 2000; Anderson et al., 2014; Waters et al., 2001) and the Defense Meteorological Satellite Program (DMSP, Paxton et al., 1993) spacecraft to analyze the FAC structure in this event. AMPERE utilizes measurements of magnetic fields by the Iridium constellation, which is composed of 66 communication satellites, to derive the FACs. DMSP contains series of sun-synchronous orbit spacecraft with orbital heights of 835–850 km. The in situ particle energy flux and magnetic field data were measured by Special Sensor for Precipitating Particles (SSJ, Hardy et al., 1984) and Special Sensor Magnetometer (SSM, Rich, 1984) onboard DMSP-F17. SSJ detects precipitating auroral ions and electrons from 30 eV to 30 keV. SSM is a triaxial fluxgate magnetometer designed to observe the magnetic signatures of FACs. The temporal resolutions of SSJ and SSM data are both 1 s. We also present spaceborne imaging data from Special Sensor Ultraviolet Spectrographic Imagers (SSUSI, Paxton et al., 1993) onboard DMSP-F18 in this letter, which provides auroral oval images in

LI ET AL. 2 of 11

121.6, 130.4, 135.6, 140–150 (Lyman-Birge-Hopfield Short, LBHS) and 165–180 nm (Lyman-Birge-Hopfield Long, LBHL) wavebands. They help us determine the relative location of the auroral curls. Using the international geomagnetic reference field (IGRF) model, we mapped the magnetic footprints of DMSP to 120 km altitude (Romick & Belon, 1967) to ensure that spacecraft observations are consistent with the ground-based imaging.

In this section, we first show observations about the spatial (latitudinal and longitudinal) structures of the auroras occurred on 23 April 2019. Then we present data relevant to the temporal structures.

#### 2.1. Latitudinal Structures

The ASI at ZHS observed multiple auroral arcs along the boundary of the southern auroral oval near the local dusk on 23 April 2019. The southernmost auroral arc suddenly brightened at around 16:11:00 UT. It further developed into series of curl-like structures between 16:12:00-16:14:30 UT (see Movie S1). Considering the similarity in morphology, we still use "curls" to refer to these auroral forms hereinafter. Figures 1a and 1b show two snapshots of the auroral curls in the 557.7 nm waveband, which are located near the eastern edge of the ASI FOV. These curls have an azimuthal wavelength of ~150 km, presenting structures like fried dough twists—a Chinese snack. However, the auroral arcs in the 630.0 nm emissions (Figures 1c and 1d) do not present curl-like structures, indicating these curls are caused by mono-energy electron precipitation. To depict the motion of the curls, we organize ASI data along the line:  $MLAT = -75.1^{\circ} + 0.0932 \times (MLON - 104^{\circ})$  in an "ewogram-like" timedependent graph (Figure 1e), where MLAT and MLON are latitudes and longitudes in altitude-adjusted corrected geomagnetic (AACGM) coordinates. The cutting line is located along the brightened auroral arc, as illustrated by the red curve in Figure 1b. The "ewogram" suggests the observed curls move westward along the arc, indicating their magnetospheric drivers propagate sunward in the dusk sector. To have a global view of the observed auroral structures, we compared the ASI image with LBHS data from SSUSI onboard DMSP-F18 during 16:30:35-16:32:43 UT (Figure 1f), which is the closest pass of DMSP spacecraft to the time when the auroral curls were detected. The result indicates the brightened arc is located near the poleward boundary of the auroral oval. Therefore, the mesoscale curls are westward-moving fine structures of the auroral oval poleward boundary.

#### 2.2. Longitudinal Structures

The multiple arcs present longitudinal quasi-periodic structures as well. We first utilized observations from AMPERE to study the distribution of FACs on a large scale. As shown in Figure 2a, the azimuthal direction of raw dB (magnetic fields measured by Iridium spacecraft minus modeled fields given by IGRF) changes when the spacecraft traveled across the multiple-arc region, indicating the direction of FAC above it is opposite to that above nearby regions. The derived FAC flows upwards above the multiple arcs and goes downwards in other latitudes (Figure 2b), consistent with the auroral arcs which result from electron precipitation.

Due to the limited spatial resolution of AMPERE data, we tried to examine the fine structures of FACs between auroral arcs using DMSP in-situ observations. Unfortunately, no available spacecraft passed through the ASI FOV when the auroral curls happened. As mentioned above, the closest pass of DMSP spacecraft took place during 16:30:35–16:32:43 UT (by DMSP-F18), but the spacecraft only crossed the edge of the FOV. Therefore, we analyzed data acquired by DMSP-F17 during the second closest pass instead, which occurred between 15:49:00-15:51:30 UT. As shown in Figure 3, DMSP-F17 traveled across the FOV at about 23 min before the appearance of the mesoscale auroral curls. The multiple-arc structure observed later has already formed at this time. Figures 3a and 3b show two snapshots of auroras in the lower-left quarter FOV of ZHS ASI, which are superimposed with DMSP-F17's magnetic footprints. For better comparison, we organize the ASI data into a "keogram" along the trajectory of spacecraft footprints (Figure 3f). The energy-time spectrogram of precipitating electron energy fluxes in Figure 3c presents "invert-V" shaped structures when the spacecraft passed through the bright arcs, suggesting these arcs correspond to precipitation of 500 eV-10 keV electrons. We transformed the measured magnetic fields into field-aligned coordinates and removed the background given by IGRF (Figure 3d), finding the azimuthal magnetic field component (positive eastward) decreases with the "invert-V" structures in Figure 3c and increases with the empty gaps between them. Using the method described in Kilcommons et al. (2017), we calculated the FAC from the magnetic field data, as presented in Figure 3e. The upward FACs agree well with the "invert-V" structures, while the downward FACs are consistent with the gaps. Through

LI ET AL. 3 of 11

19448007, 2024, 9, Downloaded from https://agupubs.onlinelibrary.wiley.com/doi/10.1029/2023GL107889 by Southwest Research Institute, Wiley Online Library on [02/04/2025]. See the Terms and Conditions (https://onlinelibrary.wiley.com/doi/10.1029/2023GL107889 by Southwest Research Institute, Wiley Online Library on [02/04/2025]. See the Terms and Conditions (https://onlinelibrary.wiley.com/doi/10.1029/2023GL107889 by Southwest Research Institute, Wiley Online Library on [02/04/2025]. See the Terms and Conditions (https://onlinelibrary.wiley.com/doi/10.1029/2023GL107889 by Southwest Research Institute, Wiley Online Library on [02/04/2025]. See the Terms and Conditions (https://onlinelibrary.wiley.com/doi/10.1029/2023GL107889 by Southwest Research Institute, Wiley Online Library on [02/04/2025]. See the Terms and Conditions (https://onlinelibrary.wiley.com/doi/10.1029/2023GL107889 by Southwest Research Institute, Wiley Online Library on [02/04/2025]. See the Terms and Conditions (https://onlinelibrary.wiley.com/doi/10.1029/2023GL107889 by Southwest Research Institute, Wiley Online Library on [02/04/2025]. See the Terms and Conditions (https://onlinelibrary.wiley.com/doi/10.1029/2023GL107889 by Southwest Research Institute, Wiley Online Library on [02/04/2025]. See the Terms and Conditions (https://onlinelibrary.wiley.com/doi/10.1029/2023GL107889 by Southwest Research Institute, Wiley Online Library on [02/04/2025]. See the Terms and Conditions (https://onlinelibrary.wiley.com/doi/10.1029/2023GL107889 by Southwest Research Institute, Wiley Online Library on [02/04/2025]. See the Terms and Conditions (https://onlinelibrary.wiley.com/doi/10.1029/2023GL107889 by Southwest Research Institute, Wiley Online Library on [02/04/2025]. See the Terms and Conditions (https://onlinelibrary.wiley.com/doi/10.1029/2023GL107889 by Southwest Research Institute, Wiley Online Library on [02/04/2025]. See the Terms and Conditions (https://onlinelibrary.wiley.com/doi/10.1029/2023GL107889 by Southwest Research Institute, Wiley Online Libr

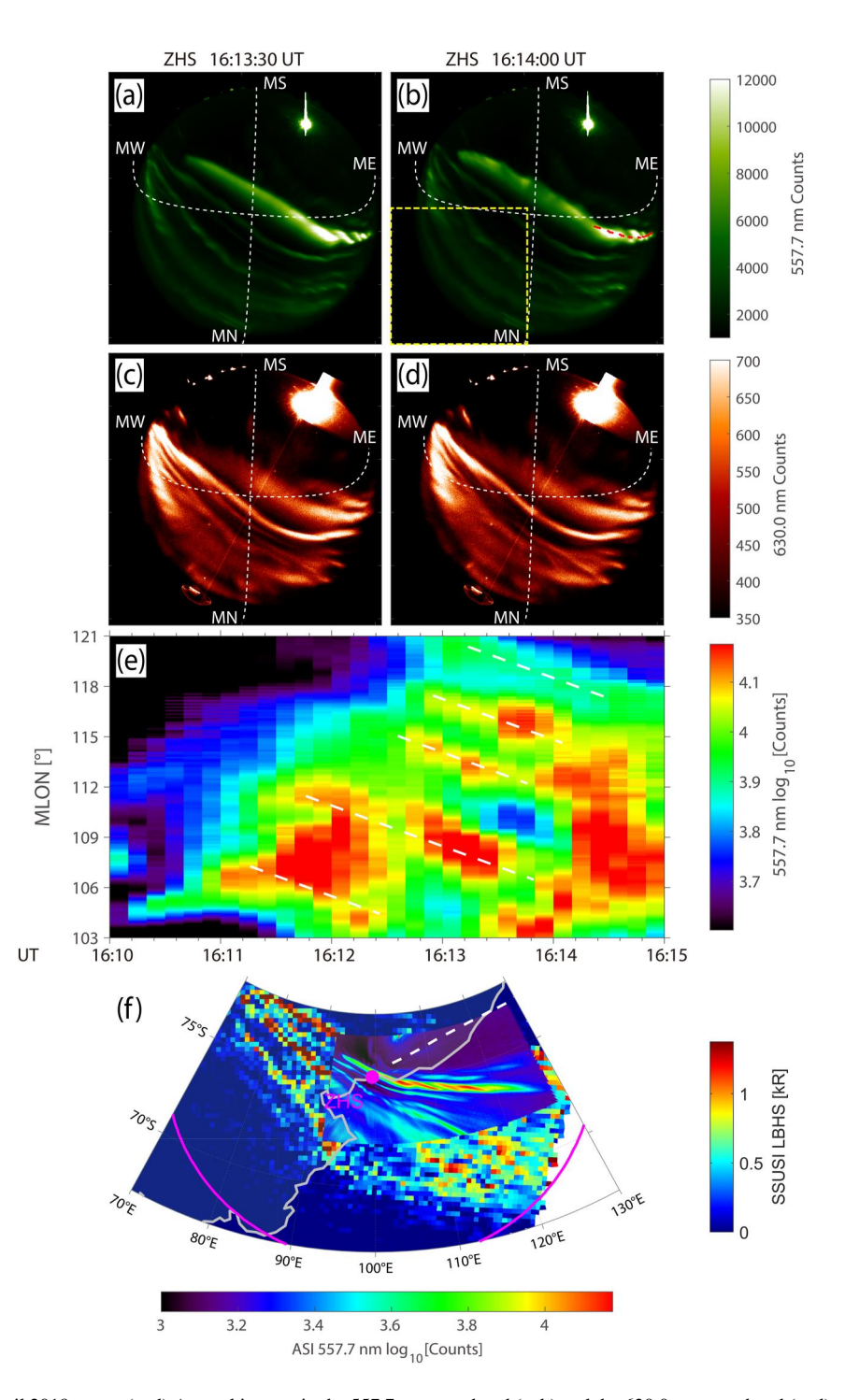
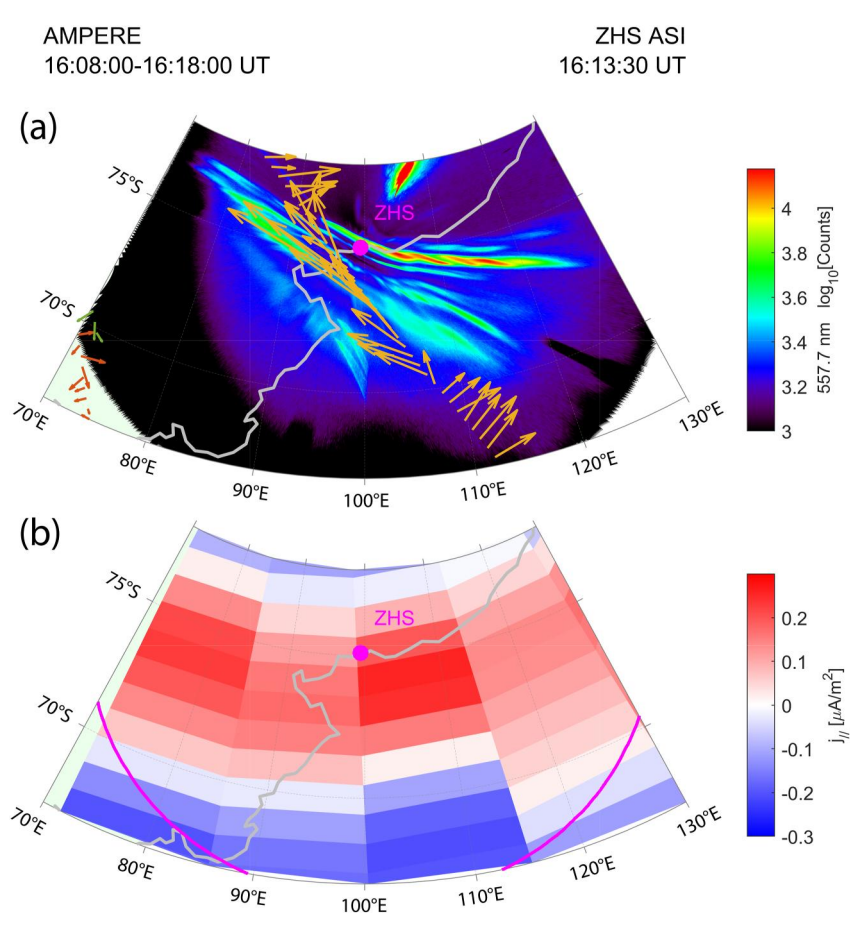


Figure 1. Overview of the 23 April 2019 event. (a–d) Auroral images in the 557.7 nm waveband (a–b) and the 630.0 nm waveband (c–d) at 16:13:30 and 16:14:00 UT, taken by the all-sky imager (ASI) in Zhongshan Station (ZHS). White dashed curves mark the latitude and longitude that cross the zenith in altitude-adjusted corrected geomagnetic (AACGM) coordinates. The yellow dashed box in panel b corresponds to the zoom-in area shown in Figures 3a-3b. (e) "Ewogram-like" time-dependent graph along the line:  $MLAT = -75.1^{\circ} + 0.0932 \times (MLON - 104^{\circ})$ , which is marked by the red dashed curve in (b). MLAT and MLON are latitudes and longitudes in AACGM coordinates. White dashed lines are used to guide the eye. (f) Lyman-Birge-Hopfield Short auroral image taken by Special Sensor Ultraviolet Spectrographic Imagers onboard Defense Meteorological Satellite Program-F18 between 16:30:35-16:32:43 UT, superimposed with the 557.7 nm auroral image captured by ZHS ASI at 16:13:30 UT. The magenta spot gives the location of ZHS and the magenta arc marks the rough boundary of ASI field-of-view. The gray curve shows the coastline of Antarctica. The white dashed line indicates the looking direction of the ZHO radar in the single-beam channel.

LI ET AL. 4 of 11

19448007, 2024, 9, Downloaded from https://agupubs.onlinelibrary.wiley.com/doi/10.1029/2023GL107889 by Southwest Research Institute, Wiley Online Library on [02/04/2025]. See the Terms and Conditions (https://onlinelibrary.wiley



**Figure 2.** Active Magnetosphere and Planetary Electrodynamics Response Experiment observations between 16:08:00-16:18:00 UT. (a) Raw dB (magnetic fields measured by Iridium spacecraft minus modeled fields given by international geomagnetic reference field) vectors along spacecraft's tracks, superimposed with the 557.7 nm auroral image captured by Zhongshan Station (ZHS) all-sky imager (ASI) at 16:13:30 UT. (b) Field-aligned currents derived from the magnetic field measurements (positive upward). The magenta arc marks the rough boundary of the ASI field-of-view. Magenta spots and gray curves in (a–b) give the location of ZHS and the coastline of Antarctica.

marking the regions above which the downward FAC flows with the magenta color in Figures 3a and 3f, we find the downward FACs correspond to the dark regions between the auroral arcs ("black auroras"). In conclusion, the multiple-arc structure indicates a series of upward-downward FAC pairs arranged in the longitudinal direction.

## 2.3. Temporal Structures

To understand the formation of the auroral curls, we also investigated the ionospheric flow field in the nearby region during this event. We used observations from the ZHO HF radar, which measures Doppler velocities of ionospheric plasma irregularities (e.g., Chisham et al., 2007). Figure 4 shows the high temporal resolution data obtained by the channel operating the single-beam (beam-07) sweep-frequency mode. The power of back-scattered signals presents signatures of been modulated (Figure 4a). To exclude the background velocity caused by plasma convection in the polar region, we removed the time-averaged value of line-of-sight (LOS) velocities for each range gate. To be more specific, we calculated the average value of the measured LOS velocity between 16:00:00–16:30:00 UT for each range. Then we subtract this value from the original velocity to detrend the data. The detrended LOS velocities are shown in Figure 4b, which oscillate quasi-periodically with periods of  $\sim$ 300 s. The frequency of the velocity variation falls in the Pc 5 band, consistent with the plasma irregularity motion driven by  $\overrightarrow{E} \times \overrightarrow{B}$  drift relevant to ULF waves in the *F* region (e.g., Shi et al., 2018; Zhao et al., 2023). The amplitude of the velocity oscillation reaches its maximum at around 16:13:30 UT (marked by the vertical black dashed line), suggesting the auroral curls are accompanied with strong plasma flows in the ionosphere.

LI ET AL. 5 of 11

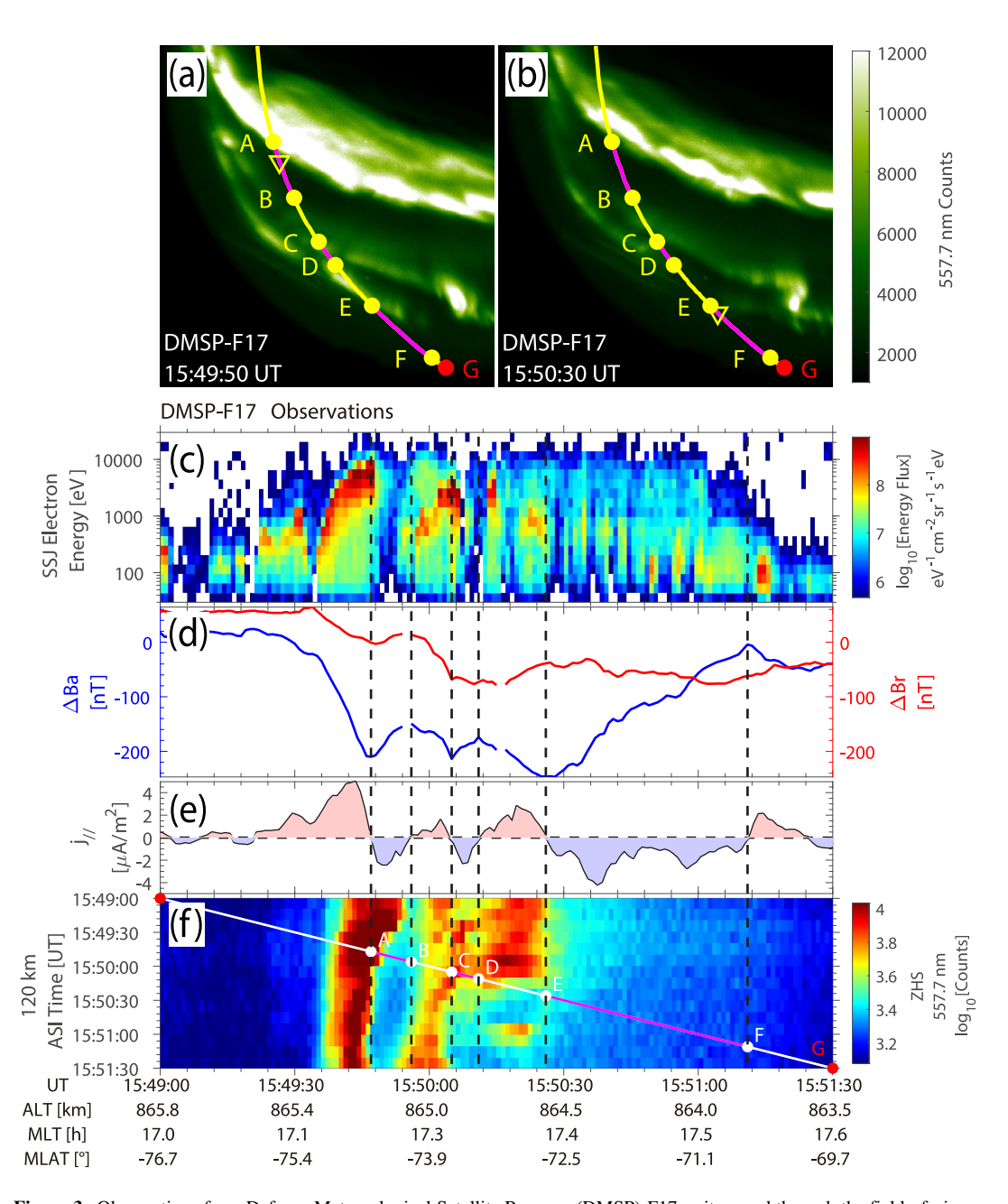


**Figure 3.** Observations from Defense Meteorological Satellite Program (DMSP)-F17 as it passed through the field-of-view (FOV) of Zhongshan Station (ZHS) all-sky imager (ASI) during 15:49:00–15:51:30 UT, which is about 23 min before the auroral curls were detected. (a–b) Auroral images in the 557.7 nm waveband at 15:49:50 and 15:50:30 UT, obtained from the lower-left quarter FOV of ZHS ASI (the yellow dashed box in Figure 1b). Yellow curves show trajectories of DMSP-F17's magnetic footprints at 120 km altitude and yellow triangles represent footprints at the time when the image was taken. The regions corresponding to downward field-aligned currents are marked with magenta curves. The letters in (a–b) represent same time with those in (f). (c) Energy-time spectrogram of precipitating electron energy fluxes, measured by Special Sensor for Precipitating Particles onboard DMSP-F17. (d) Magnetic field variations (remove background given by IGRF) in field-aligned coordinates, derived from DMSP-F17 Special Sensor Magnetometer (SSM) data. (e) FACs calculated from SSM data (positive upward) using the method described in Kilcommons et al. (2017). (f) "Keogram" along the trajectory of DMSP-F17's footprints.

LI ET AL. 6 of 11

19448007, 2024, 9, Dow.

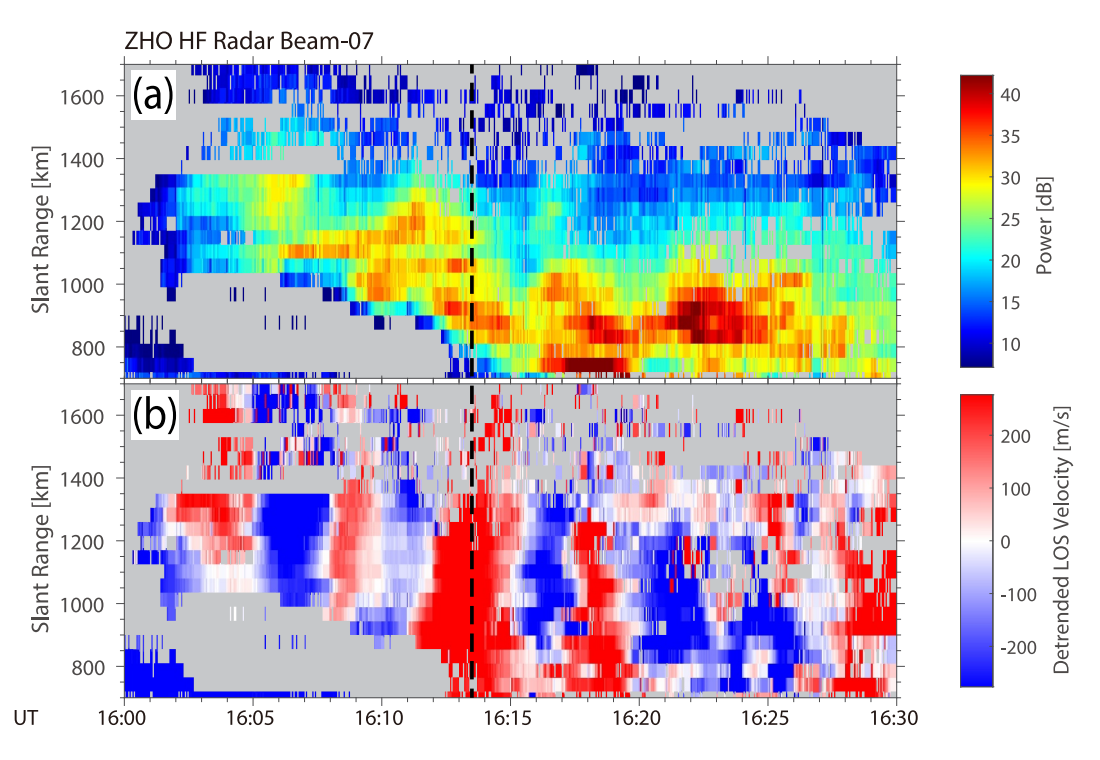


**Figure 4.** High frequency radar observations of ionospheric plasma irregularities' Doppler velocities from the single-beam (beam-07) channel between 16:00:00–16:30:00 UT at Zhongshan Station. The corresponding radar code in the Super Dual Auroral Radar Network is "ZHO." (a) The power of back-scattered signals. (b) The line-of-sight velocities detrended with the time-averaged value of each range gate between 16:00:00–16:30:00 UT. The vertical black dashed line in (a–b) marks the time when the auroral curls were clearest (16:13:30 UT).

#### 3. Discussion

#### 3.1. Brief Summary of the Observations

In this letter, we present multi-instrument observations on a new kind of auroral curls in Antarctica. Its main characteristics are summarized as follows.

- The observed auroral curls have an azimuthal wavelength of ~150 km, which are westward-moving fine structures in the poleward boundary of multiple auroral arcs.
- The multi-arc structure corresponds to a series of upward-downward FAC pairs arranged in the longitudinal direction.
- The Doppler velocities of ionospheric plasma irregularities nearby oscillate quasi-periodically with periods of ~300 s, indicating connections with ULF waves.

## 3.2. On the Formation of the Auroral Structure

The vortex-like periodic structures along auroral arcs have been investigated for decades (Kataoka et al., 2021). Previous studies have reported auroral curls resulting from the K-H instability caused by flow shear across charged field-aligned sheets (e.g., Miura & Sato, 1978). However, these structures have typical scales of several kilometers and second-order lifetimes (Hallinan & Davis, 1970; Trondsen & Cogger, 1998), much smaller than those in the discussed event. On a larger scale, auroral folds have sizes of ~20 km and lifetimes of several seconds (Dahlgren et al., 2010; Kataoka et al., 2011), which are still smaller than those observed in this event. Besides, folds are less curved than the presented structures are. Auroral spirals (e.g., Hallinan, 1976; Hu et al., 2013) have comparable spatial scales (tens to hundreds of kilometers) but different morphological forms. Meanwhile, spirals are more common in the post-midnight sector (Partamies et al., 2001), which is different from that the event occurred in (dawn sector). Conventional theories can't provide a satisfactory explanation for the reported auroral form.

LI ET AL. 7 of 11

19448007, 2024, 9, Downloaded

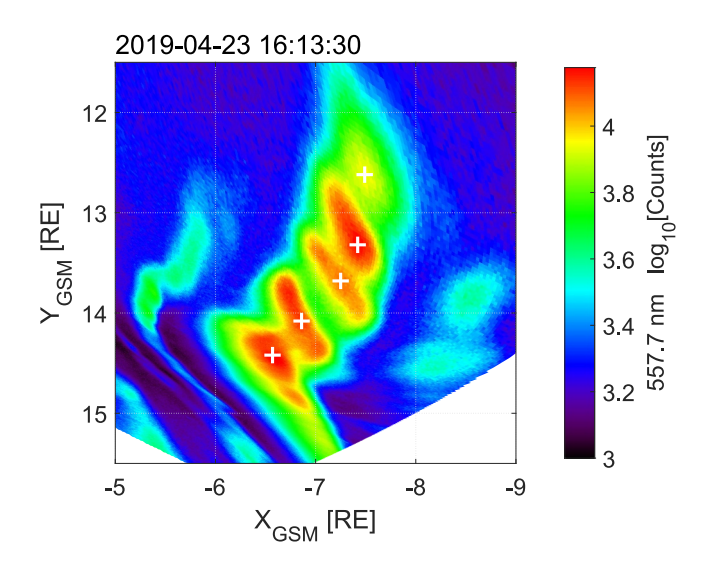


**Figure 5.** Projection of Zhongshan Station all-sky imager 557.7 nm auroral image at 16:13:30 UT on the equatorial plane of geocentric solar magnetospheric coordinates. White plus symbols mark the points utilized to calculate the azimuthal wavenumber. The magnetic field used in the projection is given by the T96 (Tsyganenko, 1995) model and the International Geomagnetic Reference Field model.

On the basis of observations, we propose these mesoscale auroral curls are connected with ULF waves in the Pc 5 band. Prior work (e.g., Cummings et al., 1969; Southwood & Hughes, 1983) has suggested that Pc 3-5 ULF waves are standing Alfvén waves along magnetic field lines. These waves propagate azimuthally, manifesting both radial and azimuthal quasi-periodic characteristics (Zong et al., 2017), which is similar to auroras in this event. Besides, the spatial and temporal scales of periodic signatures relevant to the observed curls are comparable to those of ULF waves. Using the T96 (Tsyganenko, 1995) model and the International Geomagnetic Reference Field (IGRF) model, we projected the auroral image onto the equatorial plane of geocentric solar magnetospheric (GSM) coordinates (Figure 5). The azimuthal wavelength in equatorial plane is estimated to be ~3356.27 km, which corresponds to an azimuthal wavenumber (m) of  $\sim$ -183. This value falls within the common range of m for ULF waves in observations (Zong et al., 2017). Moreover, the FAC structure self-consistent with ULF waves, as predicted by previous modeling work (Lysak et al., 2013; Southwood & Kivelson, 1991), can produce latitudinal and longitudinal periodic characteristics similar with those in the optical observations. The westward motion can also be generated by the westward propagation of ULF waves. The special "curl-like" shape may result from the superposition of multiple ULF wave modes with different azimuthal phase velocities. Another peculiarity of this event is that, these mesoscale curls are mostly significant in observations from the 557.7 nm waveband. They are nearly invisible in images from the

630.0 nm waveband (see Figure 1 in the main text and Movie S1). This signature indicates these structures also have a connection with electron pitch angle scattering caused by whistler-mode very-low frequency (VLF) waves, which can be modulated by larger-scale ULF waves (e.g., Li et al., 2023; Motoba et al., 2019). Besides, blobs of westward-moving 630.0 nm emissions (polar cap patches, Davies et al., 2002) are detected in the poleward of the arc along the poleward boundary. Data from the ZHO radar in beam-00 (the beam most closely aligned with the poleward boundary) and beam-07 show positive LOS velocities during this event (see Figure S1), suggesting the flow in the polar cap just poleward of the curls is westward. This feature is consistent with the expected direction of nightside polar cap convection for interplanetary magnetic field  $B_y > 0$  (e.g., Greenwald et al., 1995; Zhang et al., 2011), which may help us understand the westward phase velocity of the curls.

The FAC structure associated with ULF waves suggests that auroras corresponding to odd-mode harmonics are conjugate between the northern and southern hemispheres, while those corresponding to even-mode harmonics are anti-conjugate (Lysak et al., 2013; Southwood & Kivelson, 1991). However, we didn't find available observations in the northern hemisphere during the discussed event. This characteristic can be employed in subsequent studies to test the hypothesis.

In conclusion, the observed mesoscale auroral curls are different from the vortex-like periodic auroral forms in previous reports. They can't be interpreted by conventional theories and have similarities with ULF waves in both spatial and temporal structures. The results furnish a new perspective for the imaging of ULF wave activities in the magnetosphere, which is critical for comprehending the role of ULF waves in global magnetospheric dynamics. Further observational and simulation work is still needed to gain a precise understanding of these mesoscale auroral curls.

### **Data Availability Statement**

We acknowledge the Polar Research Institute of China (PRIC) for providing all-sky imager (ASI) data at the Chinese Antarctic Zhongshan Station. The ASI observations can be obtained from Li (2023). We thank the Active Magnetosphere and Planetary Electrodynamics Response Experiment (AMPERE) team and the AMPERE Science Data Center for providing data products derived from the Iridium Communications constellation, enabled by support from the National Science Foundation (https://ampere.jhuapl.edu/download/). The time intervals of interest is 2019-04-23 16:08:00–16:18:00 UT. We acknowledge Johns Hopkins University Applied Physics Laboratory for providing the Defense Meteorological Satellite Program (DMSP)-F18 Special Sensor Ultraviolet

LI ET AL. 8 of 11

Spectrographic Imagers data (https://ssusi.jhuapl.edu/data\_products/). We thank the Madrigal Database for providing DMSP-F17 Special Sensor for Precipitating Particles and Special Sensor Magnetometer data (http://cedar.openmadrigal.org/). The time intervals of interest is 23 April 2019 15:49:00–15:51:30 UT. The Zhongshan Super Dual Auroral Radar Network (SuperDARN) radar is maintained and operated by PRIC. We acknowledge the use of SuperDARN data (http://vt.superdarn.org). SuperDARN is a network of radars funded by national scientific funding agencies of Australia, Canada, China, France, Italy, Japan, Norway, South Africa, the United Kingdom, and the United States of America. The time intervals of interest is 23 April 2019 16:00:00–16:30:00 UT.

#### Acknowledgments

This work was supported by the Major Project of Chinese National Programs for Fundamental Research and Development 2021YFA0718600, the China Space Agency Project D020301, the Chinese Meridian Project, the National Natural Science Foundation of China 42130210, 42374208 and the National Key R&D Program of China 2022YFC2807205.

#### References

- Akasofu, S.-I. (1964). The development of the auroral substorm. Planetary and Space Science, 12(4), 273–282. https://doi.org/10.1016/0032-0633 (64)90151-5
- Anderson, B. J., Korth, H., Waters, C. L., Green, D. L., Merkin, V. G., Barnes, R. J., & Dyrud, L. P. (2014). Development of large-scale birkeland currents determined from the active magnetosphere and planetary electrodynamics response experiment. *Geophysical Research Letters*, 41(9), 3017–3025. https://doi.org/10.1002/2014GL059941
- Anderson, B. J., Takahashi, K., & Toth, B. A. (2000). Sensing global birkeland currents with iridium<sup>RO</sup> engineering magnetometer data. Geophysical Research Letters, 27(24), 4045–4048. https://doi.org/10.1029/2000GL000094
- Baker, G. J., Donovan, E. F., & Jackel, B. J. (2003). A comprehensive survey of auroral latitude Pc5 pulsation characteristics. *Journal of Geophysical Research*, 108(A10), 1384. https://doi.org/10.1029/2002JA009801
- Chaston, C. C., & Seki, K. (2010). Small-scale auroral current sheet structuring. Journal of Geophysical Research, 115(A11), A11221. https://doi.org/10.1029/2010JA015536
- Chen, X., Liu, J., Kosch, M. J., Hu, Z., Wang, Z., Zhang, B., et al. (2022). Simultaneous observations of a sporadic E layer by digisonde and SuperDARN HF radars at Zhongshan, Antarctica. *Journal of Geophysical Research*, 127(2), e2021JA029921. https://doi.org/10.1029/2021JA029921
- Chisham, G., Lester, M., Milan, S. E., Freeman, M. P., Bristow, W. A., Grocott, A., et al. (2007). A decade of the super dual auroral radar network (SuperDARN): Scientific achievements, new techniques and future directions. Surveys in Geophysics, 28(1), 33–109. https://doi.org/10.1007/s10712-007-9017-8
- Chmyrev, V., Marchenko, V., Pokhotelov, O., Shukla, P., Stenflo, L., & Streltsov, A. (1992). The development of discrete active auroral forms. IEEE Transactions on Plasma Science, 20(6), 764–769. https://doi.org/10.1109/27.199525
- Cummings, W., O'sullivan, R., & Coleman, P. (1969). Standing Alfvén waves in the magnetosphere. *Journal of Geophysical Research*, 74(3), 778–793. https://doi.org/10.1029/JA074i003p00778
- Dahlgren, H., Aikio, A., Kaila, K., Ivchenko, N., Lanchester, B., Whiter, D., & Marklund, G. (2010). Simultaneous observations of small multiscale structures in an auroral arc. *Journal of Atmospheric and Solar-Terrestrial Physics*, 72(7), 633–637. https://doi.org/10.1016/j.jastp.2010.
- Davies, J. A., Yeoman, T. K., Rae, I. J., Milan, S. E., Lester, M., Lockwood, M., & McWilliams, A. (2002). Ground-based observations of the auroral zone and polar cap ionospheric responses to dayside transient reconnection. *Annales Geophysicae*, 20(6), 781–794. https://doi.org/10. 5194/angeo-20-781-2002
- Davis, T. N., & Hallinan, T. J. (1976). Auroral spirals, 1. Observations. Journal of Geophysical Research, 81(22), 3953–3958. https://doi.org/10.1029/IA081i022p03953
- Frey, H. U. (2007). Localized aurora beyond the auroral oval. *Review of Geophysics*, 45(1), RG1003. https://doi.org/10.1029/2005RG000174 Gabrielse, C., Nishimura, Y., Lyons, L., Gallardo-Lacourt, B., Deng, Y., & Donovan, E. (2018). Statistical properties of mesoscale plasma flows in the nightside high-latitude ionosphere. *Journal of Geophysical Research*, 123(8), 6798–6820. https://doi.org/10.1029/2018JA025440
- Gillies, D. M., Knudsen, D., Rankin, R., Milan, S., & Donovan, E. (2018). A statistical survey of the 630.0-nm optical signature of periodic auroral arcs resulting from magnetospheric field line resonances. *Geophysical Research Letters*, 45(10), 4648–4655. https://doi.org/10.1029/2018GI 077491
- Greenwald, R. A., Baker, K. B., Dudeney, J. R., Pinnock, M., Jones, T. B., Thomas, E. C., et al. (1995). DARN/SuperDARN: A global view of the dynamics of high-latitude convection. DARN/SuperDARN. Space Sci. Rev., 71(1–4), 761–796. https://doi.org/10.1007/BF00751350
- Greenwald, R. A., Baker, K. B., Hutchins, R. A., & Hanuise, C. (1985). An HF phased-array radar for studying small-scale structure in the high-latitude ionosphere. *Radio Science*, 20(01), 63–79. https://doi.org/10.1029/RS020i001p00063
- Hallinan, T. J. (1976). Auroral spirals, 2. Theory. *Journal of Geophysical Research*, 81(22), 3959–3965. https://doi.org/10.1029/ JA081i022n03959
- Hallinan, T. J., & Davis, T. (1970). Small-scale auroral arc distortions. *Planetary and Space Science*, 18(12), 1735–1744. https://doi.org/10.1016/0032-0633(70)90007-3
- Hardy, D. A., Schmitt, L. K., Gussenhoven, M. S., Marshall, F. J., & Yeh, H. C. (1984). Precipitating electron and ion detectors (SSJ/4) for the block 5D/Flights 6-10 DMSP (Defense Meteorological Satellite Program) satellites: Calibration and data presentation (pp. 84–317). AFGL-TR
- Hu, H., Liu, E., Liu, R., Yang, H., & Zhang, B. (2013). Statistical characteristics of ionospheric backscatter observed by SuperDARN Zhongshan radar in Antarctica. *Advances in Polar Science*, 24(1), 19–31. https://doi.org/10.3724/SP.J.1085.2013.00019
- Hu, Z.-J., He, F., Liu, J.-J., Huang, D.-H., Han, D.-S., Hu, H.-Q., et al. (2017). Multi-wavelength and multi-scale aurora observations at the Chinese Zhongshan Station in Antarctica. *Polar Science*, 14, 1–8. https://doi.org/10.1016/j.polar.2017.09.001
- Hu, Z.-J., Yang, H., Huang, D., Araki, T., Sato, N., Taguchi, M., et al. (2009). Synoptic distribution of dayside aurora: Multiple-wavelength all-sky observation at yellow river station in Ny-Ålesund, Svalbard. *Journal of Atmospheric and Solar-Terrestrial Physics*, 71(8–9), 794–804. https://doi.org/10.1016/j.jastp.2009.02.010
- Hu, Z.-J., Yang, H.-G., Hu, H.-Q., Zhang, B.-C., Huang, D.-H., Chen, Z.-T., & Wang, Q. (2013). The hemispheric conjugate observation of postnoon "bright spots" auroral spirals. *Journal of Geophysical Research*, 118(4), 1428–1434. https://doi.org/10.1002/jgra.50243
- Jacobs, J., Kato, Y., Matsushita, S., & Troitskaya, V. (1964). Classification of geomagnetic micropulsations. *Journal of Geophysical Research*, 69(1), 180–181. https://doi.org/10.1029/JZ069i001p00180

LI ET AL. 9 of 11

- Jiang, W., Liu, E., Kong, X., Shi, S., & Liu, J. (2022). Zhongshan HF radar elevation calibration based on ground backscatter echoes. *Electronics*, 11(24), 4236. https://doi.org/10.3390/electronics11244236
- Karlsson, T., Andersson, L., Gillies, D. M., Lynch, K., Marghitu, O., Partamies, N., et al. (2020). Quiet, discrete auroral arcs-observations. Space Science Reviews, 216(1), 16. https://doi.org/10.1007/s11214-020-0641-7
- Kataoka, R., Chaston, C. C., Knudsen, D., Lynch, K. A., Lysak, R. L., Song, Y., et al. (2021). Small-scale dynamic aurora. Space Science Reviews, 217(1), 17. https://doi.org/10.1007/s11214-021-00796-w
- Kataoka, R., Miyoshi, Y., Sakanoi, T., Yaegashi, A., Shiokawa, K., & Ebihara, Y. (2011). Turbulent microstructures and formation of folds in auroral breakup arc. *Journal of Geophysical Research*, 116(A1), A00K02. https://doi.org/10.1029/2010JA016334
- Keesee, A. M., Buzulukova, N., Mouikis, C., & Scime, E. E. (2021). Mesoscale structures in Earth's magnetotail observed using energetic neutral atom imaging. Geophysical Research Letters, 48(3), e2020GL091467. https://doi.org/10.1029/2020GL091467
- Keiling, A., Angelopoulos, V., Runov, A., Weygand, J., Apatenkov, S. V., Mende, S., et al. (2009). Substorm current wedge driven by plasma flow vortices: THEMIS observations. *Journal of Geophysical Research*, 114(A1), A00C22. https://doi.org/10.1029/2009JA014114
- Kilcommons, L. M., Redmon, R. J., & Knipp, D. J. (2017). A new DMSP magnetometer and auroral boundary data set and estimates of field-aligned currents in dynamic auroral boundary coordinates. *Journal of Geophysical Research*, 122(8), 9068–9079. https://doi.org/10.1002/2016JA023342
- Kimball, J., & Hallinan, T. J. (1998). A morphological study of black vortex streets. Journal of Geophysical Research, 103(A7), 14683–14695. https://doi.org/10.1029/98JA00187
- Li, X.-Y. (2023). All-sky imager observations from the Chinese Antarctic Zhongshan station on April 23rd, 2019. [Dataset]. Zenodo. https://doi.org/10.5281/zenodo.10405890
- Li, X.-Y., Liu, Z.-Y., Zong, Q.-G., Liu, J.-J., Fu, S.-Y., Zhou, X.-Z., et al. (2022). ULF wave-induced ion pitch angle evolution in the dayside outer magnetosphere. *Geophysical Research Letters*, 49(8), e2022GL098108. https://doi.org/10.1029/2022GL098108
- Li, X.-Y., Liu, Z.-Y., Zong, Q.-G., Zhou, X.-Z., Hao, Y.-X., Pollock, C. J., et al. (2021). Off-equatorial minima effects on ULF wave-ion interaction in the dayside outer magnetosphere. Geophysical Research Letters, 48(18), e2021GL095648. https://doi.org/10.1029/2021GL095648
- Li, X.-Y., Zong, Q.-G., Liu, J.-J., Yin, Z.-F., Hu, Z.-J., Zhou, X.-Z., et al. (2023). Comparative study of dayside pulsating auroras induced by ultralow-frequency waves. *Universe*, 9(6), 258. https://doi.org/10.3390/universe9060258
- Liu, E., Hu, H., Hosokawa, K., Liu, R., Wu, Z., & Xing, Z. (2013). First observations of polar mesosphere summer echoes by SuperDARN Zhongshan radar. Journal of Atmospheric and Solar-Terrestrial Physics, 104, 39–44. https://doi.org/10.1016/j.jastp.2013.07.011
- Liu, J. J., Hu, H. Q., Han, D. S., Araki, T., Hu, Z. J., Zhang, Q. H., et al. (2011). Decrease of auroral intensity associated with reversal of plasma convection in response to an interplanetary shock as observed over Zhongshan station in Antarctica. *Journal of Geophysical Research*, 116(A3), A03210. https://doi.org/10.1029/2010JA016156
- Liu, W., Sarris, T., Li, X., Elkington, S., Ergun, R., Angelopoulos, V., et al. (2009). Electric and magnetic field observations of Pc4 and Pc5 pulsations in the inner magnetosphere: A statistical study. *Journal of Geophysical Research*, 114(A12). https://doi.org/10.1029/2009JA014243 Liu, Z.-Y., Zong, Q.-G., Zhou, X.-Z., Zhu, Y.-F., & Gu, S.-J. (2020). Pitch angle structures of ring current ions induced by evolving poloidal ultra-
- low frequency waves. Geophysical Research Letters, 47(4), e2020GL087203. https://doi.org/10.1029/2020GL087203
- Lysak, R. L., Waters, C. L., & Sciffer, M. D. (2013). Modeling of the ionospheric Alfvén resonator in dipolar geometry. *Journal of Geophysical Research*, 118(4), 1514–1528. https://doi.org/10.1002/jgra.50090
- Milan, S. E., Sato, N., Ejiri, M., & Moen, J. (2001). Auroral forms and the field-aligned current structure associated with field line resonances. Journal of Geophysical Research, 106(A11), 25825–25833. https://doi.org/10.1029/2001JA900077
- Miura, A., & Sato, T. (1978). Shear instability: Auroral arc deformation and anomalous momentum transport. *Journal of Geophysical Research*, 83(A5), 2109–2117. https://doi.org/10.1029/JA083iA05p02109
- Motoba, T., Ebihara, Y., Ogawa, Y., Kadokura, A., Engebretson, M. J., Angelopoulos, V., et al. (2019). On the driver of daytime Pc3 auroral pulsations. *Geophysical Research Letters*, 46(2), 553–561, https://doi.org/10.1029/2018GL080842
- Motoba, T., Ogawa, Y., Ebihara, Y., Kadokura, A., Gerrard, A. J., & Weatherwax, A. T. (2021). Daytime Pc5 diffuse auroral pulsations and their association with outer magnetospheric ULF waves. *Journal of Geophysical Research*, 126(8), e2021JA029218. https://doi.org/10.1029/2021JA029218
- Nishimura, Y., Lessard, M. R., Katoh, Y., Miyoshi, Y., Grono, E., Partamies, N., et al. (2020). Diffuse and pulsating aurora. Space Science Reviews, 216(1), 4, https://doi.org/10.1007/s11214-019-0629-3
- Oimatsu, S., Nosé, M., Teramoto, M., Yamamoto, K., Matsuoka, A., Kasahara, S., et al. (2018). Drift-bounce resonance between pc5 pulsations and ions at multiple energies in the nightside magnetosphere: Arase and MMS observations. *Geophysical Research Letters*, 45(15), 7277–7286. https://doi.org/10.1029/2018GL078961
- Partamies, N., Kauristie, K., Pulkkinen, T. I., & Brittnacher, M. (2001). Statistical study of auroral spirals. *Journal of Geophysical Research*, 106(A8), 15415–15428. https://doi.org/10.1029/2000JA900172
- Paxton, L. J., Meng, C.-I., Fountain, G. H., Ogorzalek, B. S., Darlington, E. H., Gary, S. A., et al. (1993). SSUSI: Horizon-to-horizon and limb-viewing spectrographic imager for remote sensing of environmental parameters. In R. E. Huffman (Ed.), *Ultraviolet technology iv* (Vol. 1764, pp. 161–176). SPIE. https://doi.org/10.1117/12.140846
- Rae, I. J., Murphy, K. R., Watt, C. E. J., Halford, A. J., Mann, I. R., Ozeke, L. G., et al. (2018). The role of localized compressional ultra-low frequency waves in energetic electron precipitation. *Journal of Geophysical Research*, 123(3), 1900–1914. https://doi.org/10.1002/2017JA024674
- Rankin, R., Samson, J. C., & Tikhonchuk, V. T. (1999). Parallel electric fields in dispersive shear Alfvén waves in the dipolar magnetosphere. Geophysical Research Letters, 26(24), 3601–3604. https://doi.org/10.1029/1999GL010715
- Rankin, R., Samson, J. C., Tikhonchuk, V. T., & Voronkov, I. (1999). Auroral density fluctuations on dispersive field line resonances. *Journal of Geophysical Research*, 104(A3), 4399–4410. https://doi.org/10.1029/1998JA900106
- Rich, F. J. (1984). Fluxgate magnetometer (SSM) for the defense meteorological satellite program (DMSP) block 5D-2, flight 7. In *Hanscom AFB*, *Massachusetts: Space Physics Division*. Air Force Geophysics Laboratory.
- Romick, G., & Belon, A. (1967). The spatial variation of auroral luminosity-II determination of volume emission rate profiles. *Planetary and Space Science*, 15(11), 1695–1716. https://doi.org/10.1016/0032-0633(67)90008-6
- Shi, X., Baker, J. B. H., Ruohoniemi, J. M., Hartinger, M. D., Murphy, K. R., Rodriguez, J. V., et al. (2018). Long-lasting poloidal ULF waves observed by multiple satellites and high-latitude SuperDARN radars. *Journal of Geophysical Research*, 123(10), 8422–8438. https://doi.org/10.1029/2018JA026003
- Southwood, D. J., & Hughes, W. J. (1983). Theory of hydromagnetic waves in the magnetosphere. Space Science Reviews, 35(4), 301–366. https://doi.org/10.1007/BF00169231

LI ET AL. 10 of 11

- Southwood, D. J., & Kivelson, M. G. (1981). Charged particle behavior in low-frequency geomagnetic pulsations. I—Transverse waves. *Journal of Geophysical Research*, 86(A7), 5643–5655. https://doi.org/10.1029/JA086iA07p05643
- Southwood, D. J., & Kivelson, M. G. (1982). Charged particle behavior in low-frequency geomagnetic pulsations. II—Graphical approach. Journal of Geophysical Research, 87(A3), 1707–1710. https://doi.org/10.1029/ja087ia03p01707
- Southwood, D. J., & Kivelson, M. G. (1991). An approximate description of field-aligned currents in a planetary magnetic field. *Journal of Geophysical Research*, 96(A1), 67–75. https://doi.org/10.1029/90JA01806
- Streltsov, A. V., & Lotko, W. (2008). Coupling between density structures, electromagnetic waves and ionospheric feedback in the auroral zone. Journal of Geophysical Research, 113(A5), A05212. https://doi.org/10.1029/2007JA012594
- Trondsen, T. S., & Cogger, L. L. (1998). A survey of small-scale spatially periodic distortions of auroral forms. *Journal of Geophysical Research*, 103(A5), 9405–9415. https://doi.org/10.1029/98JA00619
- Tsyganenko, N. A. (1995). Modeling the Earth's magnetospheric magnetic field confined within a realistic magnetopause. *Journal of Geophysical Research*, 100(A4), 5599–5612. https://doi.org/10.1029/94JA03193
- Vogt, J., Frey, H. U., Haerendel, G., Höfner, H., & Semeter, J. L. (1999). Shear velocity profiles associated with auroral curls. *Journal of Geophysical Research*, 104(A8), 17277–17288. https://doi.org/10.1029/1999JA900148
- Wagner, J. S., Sydora, R. D., Tajima, T., Hallinan, T., Lee, L. C., & Akasofu, S.-I. (1983). Small-scale auroral arc deformations. *Journal of Geophysical Research*, 88(A10), 8013–8019. https://doi.org/10.1029/JA088iA10p08013
- Waters, C. L., Anderson, B. J., & Liou, K. (2001). Estimation of global field aligned currents using the iridium<sup>®</sup> System magnetometer data. Geophysical Research Letters, 28(11), 2165–2168. https://doi.org/10.1029/2000GL012725
- Yamamoto, K., Nosé, M., Keika, K., Hartley, D. P., Smith, C. W., MacDowall, R. J., et al. (2019). Eastward propagating second harmonic poloidal waves triggered by temporary outward gradient of proton phase space density: Van Allen Probe A observation. *Journal of Geophysical Research*, 124(12), 9904–9923. https://doi.org/10.1029/2019JA027158
- Yin, Z.-F., Zhou, X.-Z., Hu, Z.-J., Zong, Q.-G., Liu, J.-J., Yue, C., et al. (2023). Multi-band periodic poleward-moving auroral arcs at the postdawn sector: A case study. *Journal of Geophysical Research*, 128(9), e2023JA031516. https://doi.org/10.1029/2023JA031516
- Yin, Z.-F., Zhou, X.-Z., Li, W., Shen, X.-C., Rankin, R., Liu, J., et al. (2023). Characteristics of electron precipitation directly driven by poloidal ULF waves. *Journal of Geophysical Research*, 128(3), e2022JA031163. https://doi.org/10.1029/2022JA031163
- Yue, C., Nishimura, Y., Lyons, L. R., Angelopoulos, V., Donovan, E. F., Shi, Q., et al. (2013). Coordinated THEMIS spacecraft and all-sky imager observations of interplanetary shock effects on plasma sheet flow bursts, poleward boundary intensifications, and streamers. *Journal of Geophysical Research*, 118(6), 3346–3356. https://doi.org/10.1002/jgra.50372
- Zhang, Q.-H., Zhang, B.-C., Liu, R.-Y., Dunlop, M. W., Lockwood, M., Moen, J., et al. (2011). On the importance of interplanetary magnetic field lByl on polar cap patch formation. *Journal of Geophysical Research*, 116(A5), A05308. https://doi.org/10.1029/2010JA016287
- Zhao, X. X., Zong, Q.-G., Liu, J. J., Yue, C., Zhou, X.-Z., Hu, Z. J., et al. (2023). A conjunction of Pc5 ULF waves from spaceborne and ground-based observations. *Journal of Geophysical Research*, 128(9), e2023JA031497. https://doi.org/10.1029/2023JA031497
- Zong, Q.-G. (2022). Magnetospheric response to solar wind forcing: Ultra-low-frequency wave-particle interaction perspective. *Annales Geo-physicae*, 40(1), 121–150. https://doi.org/10.5194/angeo-40-121-2022
- Zong, Q.-G., Rankin, R., & Zhou, X.-Z. (2017). The interaction of ultra-low-frequency pc3-5 waves with charged particles in Earth's magnetosphere. Reviews of Modern Plasma Physics, 1(10), 10. https://doi.org/10.1007/s41614-017-0011-4
- Zong, Q.-G., Zhou, X.-Z., Wang, Y.-F., Li, X., Song, P., Baker, D. N., et al. (2009). Energetic electrons response to ULF waves induced by interplanetary shocks in the outer radiation belt. *Journal of Geophysical Research*, 114(A10), A10204. https://doi.org/10.1029/2009JA014393

LI ET AL. 11 of 11